Optimization of Swiss used nuclear fuel canister for long-term repository: homogeneous *vs.* mixed loading

D. Rochman [a], A. Vasiliev [a], H. Ferroukhi [a], and M. Pecchia [a]

[a] *Reactor Physics and Thermal hydraulic Laboratory, Paul Scherrer Institut, Villigen, Switzerland*

Abstract

In this paper, the possibilities and advantages of loading mixed used nuclear fuel (UNF) assemblies into canisters for long-term repository are presented from a criticality aspect within the burnup credit approach (BUC). UNF coming from a Swiss reactor are taken into account at the pin-by-pin level and two canister loading patterns are studied: mixed and homogeneous (*i.e.* mixing UNF with various burnup values and enrichments, or not). The advantages of the mixed cases are presented in terms of criticality, together with the impact of assembly axial and radial rotations. The main outcome of the mixed loading is that a variety of UNF assemblies can be safely loaded together, including those which were previously not allowed in the homogeneous case.

Key words: spent nuclear fuel, repository, canister optimization, criticality

1 Introduction

The safe storage of used Nuclear Fuel (UNF, also called spent nuclear fuel) for long-term repository is one of the highest priorities for the back-end of the fuel cycle for countries avoiding reprocessing. Many aspects have to be considered to ensure that during hundreds of thousands of years, the UNF will not be a danger for the environment: deep storage (typically below 300 m), no human maintenance, radiation barriers, migration barriers, integrity, *etc.* Additionally, given the high cost of the repository facility including canisters containing the UNF, various degrees of storage optimization can naturally be considered. As of today, the strategy for such repository is handled at national levels (with strong support of international organizations and specific European funding), but often technical solutions and possibilities are shared

among concerned countries (to mention only a few: Sweden [1], Finland [2], Germany [3], Switzerland [4–8]).

One important phenomenon which needs to be under control is the criticality aspect of such UNF canisters, defined by the k_{eff} quantity: the effective neutron multiplication factor (if k_{eff} is greater than 1, the number of neutrons produced by the configuration will increase and lead to a diverging chain reaction). Therefore a safety requirement for a canister filled with UNFs is that its k_{eff} is lower than a certain value for the full storage period, including for instance flooding and deformation possibilities [7]. Taking into account an additional safety margin, the administrative limit considered during the present study is not 1 but 0.95, neglecting different sources of uncertainties.

In the present work, we will focus on the calculation of such k_{eff}, keeping in mind that other safety criteria are taken into account during the assessment of a specific canister configuration, for instance the decay heat. In Refs. [6–8], studies of k_{eff} variations for various canister and loading configurations were presented: the canister model (geometry, wall materials) was fixed, and the UNF contents (from a Pressurized Water Reactor, or PWR) were varied to account for burnup in order to calculate k_{eff} values. For instance, considering that each canister can be filled with 4 UNF assemblies, it was studied how k_{eff} varies as a function of the initial fuel enrichments and assembly average burnup values for various cooling times. Such studies have led to so-called "loading curves", defining which assemblies can be safely loaded in a canister for long-term storage (allowed configurations), and which not (forbidden configurations). For example, it was shown that for four identical assemblies with an initial enrichment of 3.5 % in ^{235}U and an assembly burnup value of 10 MWd/kgU, the k_{eff} can be higher than 0.95 with conservative assumptions. On the contrary, for the same enrichment and an assembly burnup value of 30 MWd/kgU, the k_{eff} will not be higher than 0.95, leading to an allowed assembly loading.

In Refs. [6,7], the decision to apply a conservative approach was taken to obtain the most penalizing configurations. A few simplifications were considered in order to have a first and conservative assessment of such loading curves. The main one is the homogeneous loading, *i.e.* using four identical assemblies (same enrichment, and same burnup value). This helps to simplify the approach to a limited number of parameters per canister: one enrichment, one burnup value and one maximum k_{eff} reached at a particular storage time. Other conservative approximations were done regarding the assembly burnup profiles (radial and axial) and the calculation of the isotopic contents (see these references for details). Ref. [8] considers a non-conservative approach by extracting the fuel content for each node from a three-dimensional core calculation using the SIMULATE and *SNF* codes [9,10]. In these three references [6–8], the fuel contents were used to build a pin-by-pin Monte Carlo model (with MCNP [11]) to calculate k_{eff} for the loaded canister (with the use of an in-house tool called COMPLINK [12]).

In the present study, we propose to go beyond the main previous limitations

and to consider four different assemblies loaded per canister, also called a mixed loading using the CS_2M method [8]. This will simulate the reality in a closer manner, while retaining the "lessons learned" from the previous studies. The fuel content of these assemblies will also come from three-dimensional core calculations, transferred to a pin-by-pin Monte Carlo model for k_{eff} calculation. As presented later, once the selection of four different assemblies is done, more than a single k_{eff} value can be obtained for a specific storage time: because of the burnup gradients inside each assembly, the loaded canister k_{eff} value can strongly vary following the relative position of each assembly (relatively to each other, but also considering assembly axial and radial rotations). As a representative example, the loading of a set of four different assemblies only in a single canister can lead to more than 93 000 configurations, each of them having different k_{eff} values, over a spread reaching a few thousands of pcm (1 pcm=10^5), depending on the assembly burnup values. This is the main difference compared to an homogeneous loading based on assembly irradiation calculated with infinite boundary conditions: the relative positioning does not matter.

We will then demonstrate that considering realistic cases and mixing assemblies (from both the allowed and forbidden zones) offers the possibility to safely load them from a criticality point of view, therefore optimizing the loading strategy. One of the positive outcomes might be a more efficient use of canisters (always filled with the maximum number of UNF), lower k_{eff} values, or higher homogeneity between canister k_{eff} values for a full park of hundreds of canisters. But this comes at a cost: more simulations, knowledge of the real assembly irradiation life, and a follow-up of each single assembly which might be difficult in practice. Finally, the possibility to have some assemblies axially rotated ("bottom-up") might also not be practically feasible.

In the following, the canister and assembly models are first presented, followed by the k_{eff} calculations for homogeneous loadings. In a second part, the mixed loading is presented with a few examples. As demonstrated, it will allow to combine assemblies with low and high burnup values, still obtaining a k_{eff} lower than 0.95 for specific axial and radial assembly combinations.

Finally, one of the motivations to perform this study lies in the believe that optimization is a crucial and necessary stage towards a more efficient management of our resources. We refer to the following interview from Ref. [13] which summarizes well the context:

Journalist Hearing you say you're getting into this because there's more bang for your buck is not inspiring, Bill.

Bill That's too bad, you know it's not my goal to be inspiring. The world has limited resources.

Journalist So if you're not doing things to be inspiring, what are you doing for?

Bill Optimization

As a final remark, the present work is performed within the long-term goal of developing an independent integral methodology for "best-estimate plus uncertainties" spent fuel analysis. It is designed to supplement existing approaches currently under development, such as BUC [14]. It will also open perspectives for loading optimization when considering a full national canister park.

As mentioned in the introduction, a number of countries are studying for several years various possibilities for safe transportation and long-term storage of UNF, either with different containers (cask and canister), or with multi-purpose canisters. The traditional approach for filling such containers is to assume the same characteristics for all assemblies, defined as homogeneous loading [15].
Up to now, the mixed loading was not considered as it departs from practices based on conservatism, as presented in following studies: in Sweden [16], Finland [17,18], Japan [19], France [20], USA [21] and Switzerland [6]. But the notion of mixed loading was nevertheless already considered as a way to simultaneously load UO_2 and MOX assemblies [7], lower the decay heat [22], or simultaneously store assemblies from boiling and pressurized water reactors [23]. As presented in the following, the continuation of the analysis of mixed loading possibilities is therefore logical outside the conservative assumptions.

2 Canister and assembly models

All simulations are performed with the same canister model, but the loaded assemblies, positions and orientations will vary from one calculation to another in the case of mixed loading. This section briefly describes the canister, with a stronger emphasis on the assembly models and the origin of the fuel content.

2.1 Simulation tools

The present study follows the approach proposed in Ref. [8], called the CS_2M method and differs from Refs. [6,7] by (1) not applying conservative assumptions, and (2) using a three-dimensional core simulator to calculate the UNF content. CS_2M is built on the four following codes: CASMO, SIMULATE, *SNF* and MCNP [9–11,24]. It is based on validated models for CASMO and SIMULATE leading to more realistic assumptions (such as for the irradiation histories, radial and vertical burnup profiles). At PSI, a validated database was built over the past years for three-dimensional steady-state core analysis for Swiss reactors (called CMSYS [27]). Such database contains models for

the two-dimensional fuel assembly depletion code (with pre-defined matrix of history and branch calculations) CASMO and the three-dimensional core analysis code SIMULATE. These models are validated against plant measurements (in the case of PWR: boron concentrations and transverse fission rates) and are at the basis of the work performed in this paper. Without this crucial information from the power plant operations, the CS_2M method could not be applied. In summary, the following calculation path is performed (see Ref. [8] for more details):

- CASMO and SIMULATE. CASMO is used to generate matrices of data for SIMULATE. Assembly models are built using information from the fuel vendor and generate multigroup cross sections and discontinuity factor data for SIMULATE. SIMULATE is a two-group nodal code used in this context for three-dimensional core cycle calculations.
- *SNF*. Once cycle calculations have been performed with SIMULATE, the information for the assembly irradiation history can be extracted and used to provide the isotopic composition for each fuel rod and vertical segment by *SNF*. It provides the isotopic content for the main actinides and important fission products, based on the pin burnup profile provided by SIMULATE and the macroscopic cross section library from CASMO. In this study, only the actinide concentrations are transferred to the Monte-Carlo transport code; the fission products are not taking into account to maximize the k_{eff} values, following the actinide-only burnup credit methodology [25,14].
- MCNP. The isotopic content for each rod and segment is used to build a pin-by-pin three-dimensional model for a Monte Carlo transport code. The translation from the *SNF* output to the transport code is performed by COMPLINK. In Ref. [8], MCNP was used, whereas in this work, the SERPENT code [26] is selected for the calculation of k_{eff}. The convergence of the k_{eff} calculations was checked and the neutron population is set to reach a statistical uncertainty of 10 pcm.

Using the CMSYS database, all the assemblies can be followed during their irradiation life, providing all the necessary information to build accurate models. An example for the irradiation life of two similar assemblies is presented in Fig. 1. Two specific assemblies are represented by the blue and yellow dots, over an irradiation of four consecutive cycles. These two assemblies are similar: same geometry, same enrichment (4.3 %) and irradiated during the same cycles. At the end of each cycle, their average burnup values are very similar (see the numbers provided in Fig. 1). Nonetheless, these assemblies are located at different positions during the four cycles and therefore the boundary conditions are different. This impacts the fuel contents and examples are presented on the right two columns of Fig. 1: colors for each rod are proportional to the fissile content for the central assembly segment. Here, the term "fissile" is simply the sum of the ^{235}U, ^{239}Pu and ^{241}Pu contents as the end of each cycle. In this figure, the blue and red colors for each pincell indicate low and high

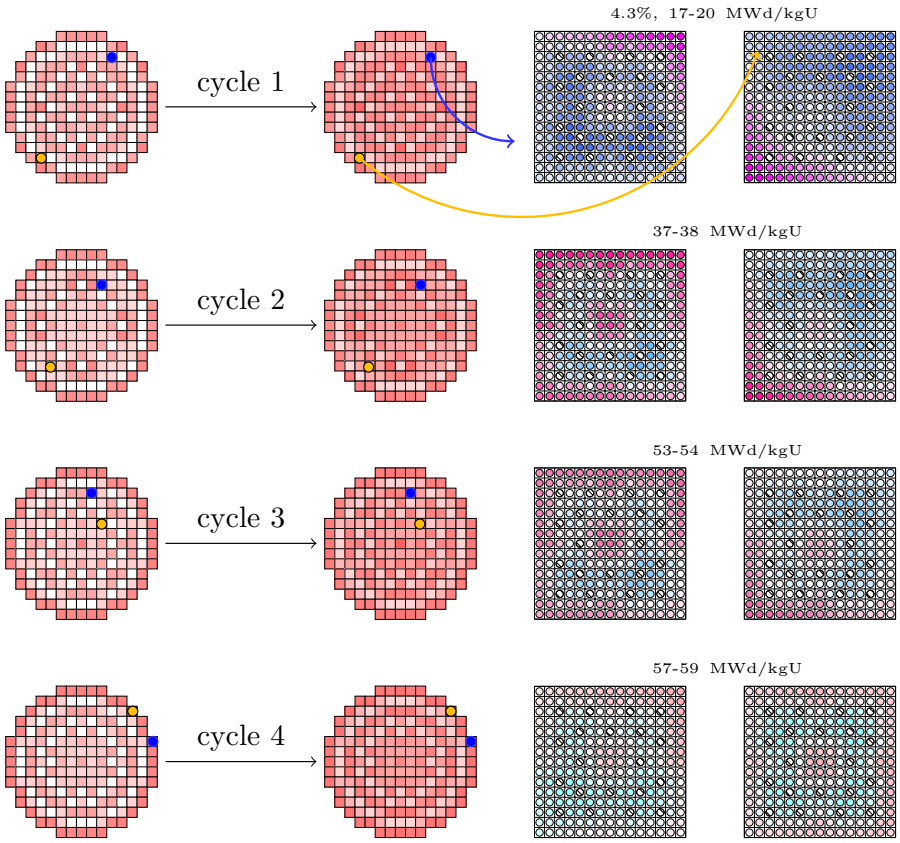

Fig. 1. Example for the irradiation history of two similar assemblies (same enrichment and similar final average burnup), irradiated during the same cycles, but leading to two different fissile content distributions. See text for details.

concentrations, respectively.

This example indicates the importance of following the irradiation history of specific assemblies to obtain an accurate fuel rod content. Considering that these assemblies have the same pinwise fuel content because they have the same average burnup and enrichment would lead to a biased estimation of (at least) one of the assembly content, and impact the calculation of the canister k_{eff} value.

2.2 Canister and assembly models

The *SNF* code is used to compute the isotopic concentrations for a specific assembly at the end of cycle, for each rod and for a number of vertical segments. As the amount of data is relatively large, the in-house utility COMPLINK is used to extract the information from the *SNF* output files and build a pin-by-pin SERPENT model. Typically, for the assemblies used in the following, the number of fuel zones per assembly is about 8200 (205 rods with 40 axial

segments). Considering that four assemblies are loaded in the canister, a typical size for the SERPENT input file is 25 Mb (more than 800 000 lines) for actinides-only fuel content.

The canister model is based on a preliminary Swiss disposal canister design [28,29]: the cask is made of carbon steel cylinder, containing four assemblies in the case of PWR UNF, separated by carbon steel boxes. For the present study, the canisters are also considered flooded with water and not deformed. A simplified representation is presented in Fig. 2. For details, see

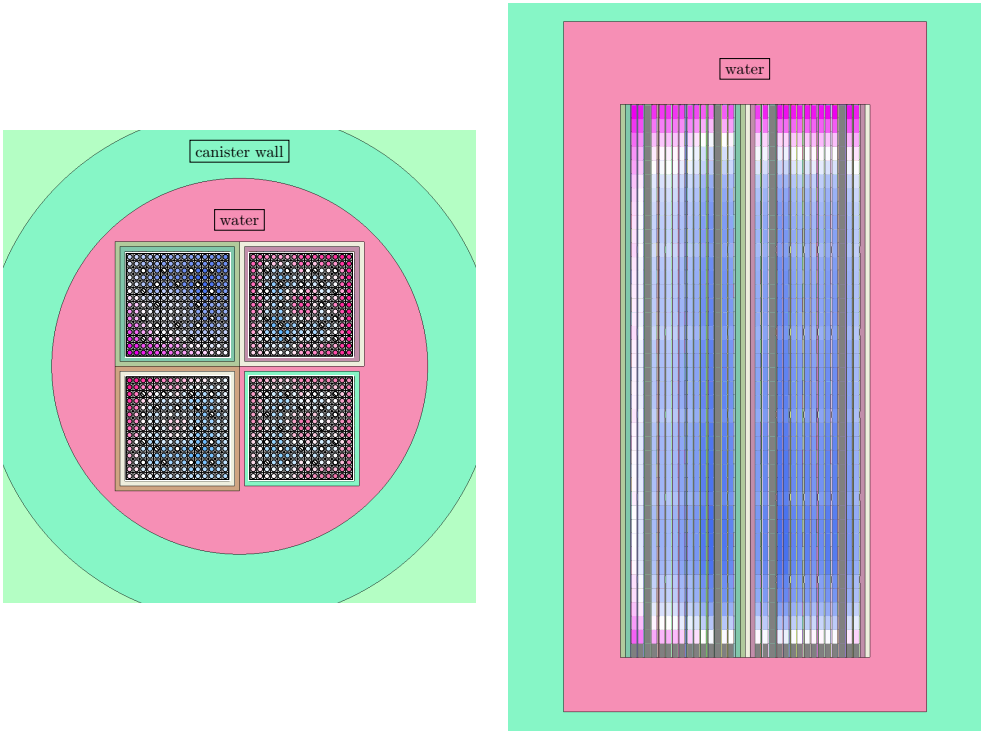

Fig. 2. Geometry of a representative canister with four assemblies for PWR assemblies. Left: radial cut at the center of the canister; Right: vertical view cutting the raw of rods on the 6^{th} column. The colors for the fuel zones are proportional to the fissile content: red for high content, blue for low and white for average, as done in Fig. 1.

Ref. [7]. As observed, a detailed pin-by-pin description of each assembly is taken into account. For the present study, all the UNF assemblies used in this work come from the Gösgen reactor cycles. The fuel is made of UO_2, with an array of 15×15 pins, including 20 guide tubes. Note that the assemblies are not located at the center of the canister: there is more (water) space at the top of the canister compared to the bottom. This will influence the k_{eff} calculations as presented in section 3.

Additionally, the radial and axial burnup profiles for each pin are directly obtained from the SIMULATE calculations. An example for the radial profile of a central segment (segment 20) is presented in Fig. 2 for the fissile contents of each pin. As observed, each assembly presents a specific radial profile due

to its own irradiation history and its location in the various cycles. In Fig. 2, the colors of each pin are proportional to the fissile concentration: light blue for low concentrations and dark red for higher concentrations (the colors are normalized to the fissile content per assembly). For the present study, the case of various assemblies will be detailed. Although the k_{eff} varies as a function of cooling time, only one cooling time will be considered here for simplicity: the isotopic content of all assemblies will come after a short cooling period of 0.1 year after a specific cycle. In the case of UO_2 fuel, it was shown in Refs. [6,7] that one of the highest k_{eff} is obtained shortly after the last irradiation. Finally, the present study is performed considering the case of "actinides only": *i.e.* that fission products are not considered for the criticality calculations.

3 Assembly loadings and criticality values

Considering one type of Swiss reactor for the purpose of this study, there are still a large number of UNF assemblies to be loaded in canisters. The optimization of canister loading for a large number of assemblies and canisters is not considered in this work, but is nonetheless an interesting subject of research [30,23,31]. In the framework of defining loading curves, we will study here a limited number of UNF assemblies. Thus the optimization will focus on the gain from using mixed loadings with various axial and radial rotations, compared to the homogeneous loading. Following the definitions of the previous references, we also will present the "loading curves" for homogeneous loading in two specific cases: one without considering any rotation (radially and axially) and using four times the same assembly (case 1), this case will therefore be similar to Ref. [8]; and one case still using four times the same assembly, but with axial and radial rotations (case 2).
The definition of two specific terms needs to be recalled for the understanding of the following study: permutation and combination. Combination is a selection of members regardless of the order. Permutation is the same but taking into account the order of the selections. In the following, a canister can be filled with 4 assemblies, therefore considering p assemblies, the number of permutations is $P(p,4) = p!/(p-4)!$ and the number of combinations is $C(p,4) = p!/(4!(p-4)!)$.

3.1 Homogeneous loading

The homogeneous loading is defined to obtain a simplified representation of the canister loading possibilities. By taking into account four times the same assembly in a canister, a limit between allowed ($k_{eff} < 0.95$) and not allowed ($k_{eff} \geq 0.95$) loadings can be established as a function of two parameters: the

assembly enrichment and burnup values. A unique and conservative axial and radial rotation is considered in Refs. [6,7] and more realistic ones in [8]. This last option is presented in Fig. 3 as "Case 1". The four assemblies are the

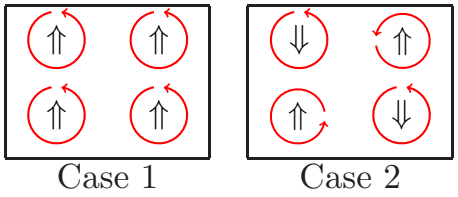

Fig. 3. Representation of the orientations of the four assemblies in both homogeneous cases 1 and 2. See text for details.

same, not rotated (the double arrows indicate the axial rotation, the circular arrows the assembly radial rotation, and their colors the assembly characteristics, being the enrichment and assembly burnup values). In the homogeneous loading, all colors are the same (red in Fig. 3), but for mixed loadings, the colors can differ for each assembly (see next section). While considering realistic burnup profiles and homogeneous loadings, one can still axially and radially rotate these assemblies, as presented in "Case 2" of Fig. 3. Such changes can potentially change the calculated k_{eff} value compared to "Case 1" because of the asymmetric radial burnup profile of each assembly. A limited number of assemblies are considered compared to Ref. [8], but still more than in Ref. [7]. In total, 8 enrichments are selected (from 1.90 % to 4.3 %) for 49 assemblies (various assembly burnup per enrichment). Fig. 4 presents such loading curves for UO_2 fuel using the model presented in Fig. 2. Both curves (lines) from case 1 and 2 are overlapping, indicating that in the case of homogeneous loading, the effect due to the radial and axial rotations is not important. The curves

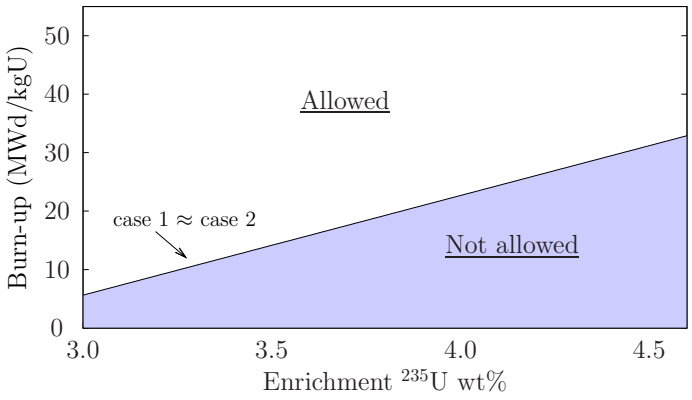

Fig. 4. Example of the loading curves (overlapping black lines separating both zones) for UO_2 assemblies as defined in Refs. [6–8] (*i.e.* homogeneous loading: four times the same assemblies).

differ a little compared to Ref. [8] because of some simplifications in the geometry model and differences for the distances between assemblies. If a given assembly has a specific enrichment and average burnup which correspond to the zone below one of the curves, then its loading (following the definition of

homogeneous loading, or four times the same assembly in the canister) is not allowed. On the contrary, if an assembly has its two characteristics (enrichment and burnup) in the part above the curves, then the homogeneous loading is allowed.
Concerning the differences between case 1 and 2, the effect of the orientation is weak for configurations with high k_{eff}: a reduction of about 100 pcm is possible in case 2 for $k_{eff} \approx 0.95$; on the contrary, the effect is larger for low k_{eff}: up to 2500 pcm can separate case 1 and 2. But for the calculation of the loading curve, the region in the vicinity of $k_{eff} \approx 0.95$ counts, the impact of the radial and axial rotations is therefore negligible for the homogeneous loading. This nevertheless indicates that a gain of reactivity is possible, but not for homogeneous loadings.

3.2 Mixed loading

A mixed loading of assemblies represents a different loading option. Instead of considering four times the same assemblies, different ones are loaded in a canister. They can have the same burnup and enrichment values, same burnup but different enrichments, or different burnup and enrichment. In Fig. 4, these mixed assemblies would be distributed in various parts of the graph. To symbolize such loadings, one assembly corresponds to a specific color in Fig. 5: a loading with four colored assemblies means that each assembly has at least a different value for the enrichment and (or) its burnup.
Similarly, their relative emplacement in the canister and rotation can influence the k_{eff} due to different burnup profiles. Three examples are presented in Fig. 5. It is then intuitive to understand that loading curves as defined in

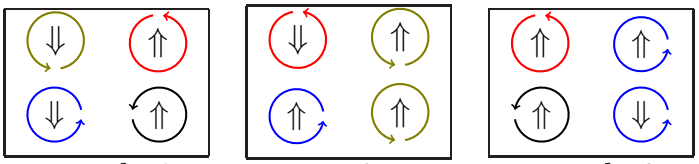

Fig. 5. Example of representations of the orientation of four assemblies in mixed loadings. The double central arrow indicates if the assembly is axially inverted. The circular arrows indicate the radial rotations.

the homogeneous loading are not appropriate. In the following sections, examples of various scenarios will be presented to show the advantage of the mixed loading: there exist solutions (loading patterns) combining allowed and not allowed assemblies (from the homogeneous loading definition) leading to $k_{eff} < 0.95$.

3.2.1 Considered mixed cases

To illustrate this study, five different loading cases are considered, named A to E. Their main characteristics are presented below.

-A- 4 assemblies in the "not allowed" region (Fig. 4), all 3.81 % ^{235}U, with similar burnup values of about 14.5 MWd/kgU.
-B- 4 assemblies in the "allowed" region, all 3.81 % ^{235}U, with similar burnup values of about 42.5 MWd/kgU.
-C- 8 assemblies: from A and B. It is a mixture of assemblies from both "allowed" and "not allowed" regions.
-D- 9 assemblies: all 4.30 % ^{235}U, with burnup values of 11.8, 15.9, 19.5, 27.8, 28.0, 35.6, 40.8, 47.5 and 53.0 MWd/kgU. Among them, three are in the "not allowed" region, four in the "allowed" region and two very close to the loading curve.
-E- 8 assemblies named e1 to e8: various enrichments and burnup e1:(3.5 %, 10.2 MWd/kgU), e2:(4.30, 11.8), e3:(3.81, 14.8), e4:(4.10, 15.2), e5:(3.80, 20.6), e6:(3.50, 33.4), e7:(4.28, 34.5) and e8:(3.81, 42.6). e1 to e4 are in the "not allowed" region and e5 to e8 in the "allowed" region.

In case A, all assemblies have a similar burnup and the same enrichment. They were irradiated under different conditions and therefore can have different burnup profiles (as presented in Fig. 1). If each of them would be considered in homogeneous loading, they would be in the "not allowed" zone.
The second considered case, case B, is similar to A but with a higher burnup of about 42.5 MWd/kgU, locating these assemblies in the "allowed" zone in Fig. 4. Case A (as well as case B) can fit in a single canister as four assemblies are considered. Case C is a mixture of A and B: it represents 8 assemblies: 4 from each loading zone. These 8 assemblies would then fit in two canisters. Case D is made of 9 assemblies with different burnup and the same enrichment values, some of them being in the allowed zone, others not. Finally case E is made of 8 assemblies with various enrichments and burnup values. This is the closest case to a fully mixed option.
The goal of such selection (especially C, D and E) is to answer the following question: can each case be loaded in one or two canisters with a k_{eff} lower than 0.95 ?
As it will be demonstrated, a large range of k_{eff} can be obtained, and a number of them are below 0.95. In the next section, the k_{eff} values for each case from A to E will be presented. As the SERPENT calculations are time consuming (about 2 hours on a single node with 36 cpu), only a few thousands of permutations will be considered, still showing the spread of the results, and including acceptable loading cases.

3.3 Results of mixed loading

The results for the five cases (A to E) are presented in this section. Cases A and B can be considered close to homogeneous loading, as the enrichments and burnup values are similar. Cases C, D and E are more complex examples, showing the potential gain in using a mixed loading.

3.3.1 Weak rotation effects: cases A, B and C

Fig. 6 presents the k_{eff} distributions for cases A, B and C. The scattered data are the calculated k_{eff} for specific canister loadings. As mentioned before, not all permutations are calculated, but a random selection of more than 1000 loadings per case is performed. In case A, the impact of the axial and radial rotations is rather limited, with a total spread of k_{eff} of about 360 pcm. This is consistent with Fig. 4 where the loading curve is not affected by these rotations. Three groups of values can be observed and are directly correlated with the orientations of the assemblies: the highest k_{eff} group is obtained when all assemblies are in the same axial direction, with the highest fissile content at the top of the canister. Within this k_{eff} group, an additional spread is obtained from the radial rotations. The second group is obtained when all assemblies are axially rotated (highest fissile content at the bottom of the canister). These differences are due to the fact that the assemblies are not located at the axial center of the canister, but lower (more water content at the top of the canister). Additionally, these high k_{eff} values are obtained when all assemblies are facing towards the same axial direction. The lowest (and most populated) k_{eff} region concerns permutations of axially and radially rotated and not rotated assemblies. In conclusion of case A, the radial and axial rotations do affect the k_{eff}, but in a limited manner, noting that all values are above 0.95 with a maximum spread of 360 pcm (radial and axial effect), and about 70 pcm for the axial rotation and 50 pcm for the radial rotation alone. Case B is very similar to case A, but the k_{eff} values are relatively low due to the higher burnup of the assemblies. The total spread of the permuted cases is about 1600 pcm (axial and radial rotations), sensibly higher than for case A. The effect of the radial rotations is also very limited with a maximum impact of about 100 pcm. Such a spread, if assemblies from A and B are loaded together, will help to reduce the k_{eff} values as demonstrated in case C. Such case can be relevant for the last cycle of a plant, where assemblies with low and high burnup values will be available at the end of cycle.
Case C is the combined loading of assemblies from cases A and B. These 8 assemblies would therefore fit in two canisters. As observed in Fig. 6, very distinct groups of k_{eff} values are obtained. At the extreme high and low k_{eff}, one can recognize the cases A and B: these values are obtained if one of the canister is filled only with assemblies from A or B. In this case, one canister

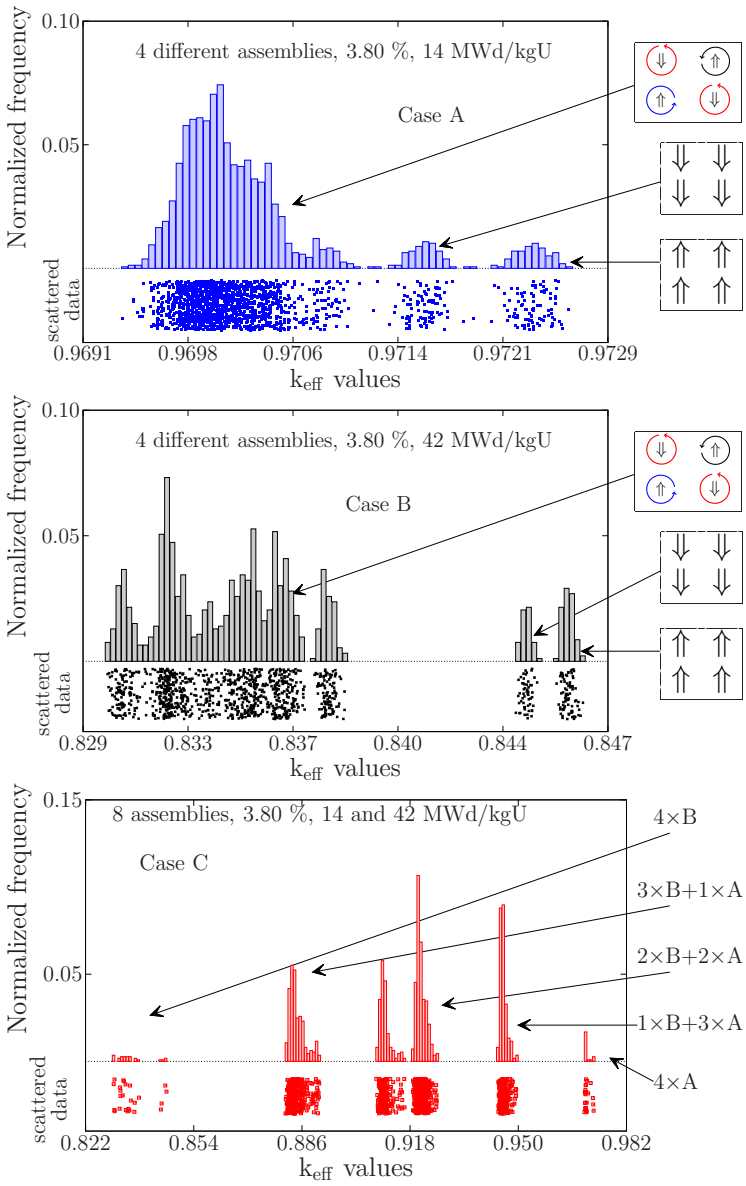

Fig. 6. Distribution of the k_{eff} for various permutation possibilities of canister loading considering cases A, B and C. The symbolic pictures on the right represent the axial and radial rotations for each k_{eff} group.

would have a k_{eff} lower than 0.95 (case B) and one higher (case A). In between are the loadings where A and B are mixed: the more A assemblies loaded in the same canister, the higher its k_{eff}. An acceptable compromise is found when two assemblies from A are mixed with two assemblies from B (see the k_{eff} values close to 0.92). In this case, both canisters have a k_{eff} lower than 0.95. The axial and radial rotations are not the first contributors to the k_{eff} variation: see the spread around each of the 6 peaks due to the assembly rotations, increasing from high to low k_{eff} values.

In conclusion of these 3 cases, mixing assemblies lead to combinations with k_{eff} lower than 0.95. But the assembly rotations represent a k_{eff} variation of

second order.

3.3.2 Strong rotation effects: cases D and E

Cases D and E increase the variability of the assemblies by considering various burnup values for a unique enrichment (D) and also for various enrichments (E), see Fig. 7 (top). Some of the assemblies are in the "allowed" region and

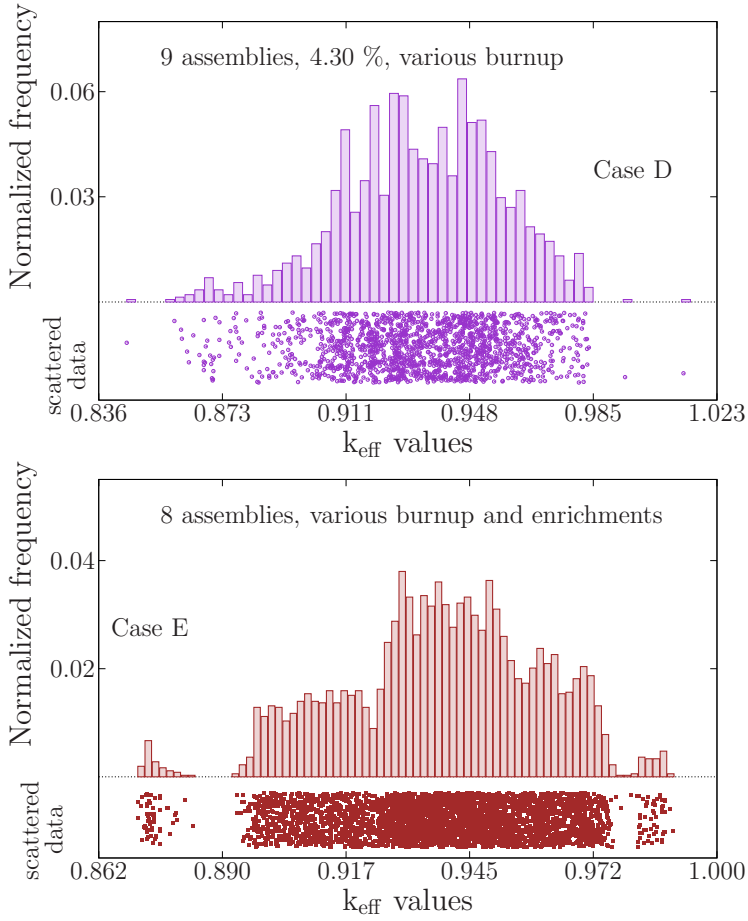

Fig. 7. Distributions of k_{eff} for the various possibilities of canister loading considering cases D (top) and E (bottom).

others are not: by considering homogeneous loading, a number loading possibilities lead to k_{eff} lower than 0.95.

For case D, among the 126 combinations of four groups with 9 assemblies, only 85 were calculated with various rotations due to the limited number of sampling performed (1570 cases were run). Out of these 85 combinations, 74 present loading possibilities with $k_{eff} < 0.95$. This confirms the advantage of the mixed loading: a large number of combinations is satisfying the k_{eff} criteria. Therefore all assemblies can be loaded if they are correctly selected and positioned in each canister.

Contrary to the previous cases (A to C), the axial and radial rotation effects

can be important for these D loadings. The total spread due to the radial and axial rotations can be as low as a few hundreds pcm (difference between the minimum and maximum k_{eff} for a selection of four assemblies) and up to 2000 pcm. The separated effects of the radial and axial rotations are also widely varying: from 400 to 2000 pcm for the axial effect, and from 10 to 1000 pcm for the radial effect. A tendency of the change in the rotation effect as a function of a specific parameter (such as the averaged loaded burnup) was not observed. Case E is similar for the distribution of k_{eff} and the impact of the rotations. Results are presented in Fig. 7 (bottom) with about 2200 random loadings. One can see a structure with three peaks: one below k_{eff} of 0.89, one above 0.98 and one in between with the majority of the values. The lowest peak corresponds to permutations of the four assemblies with the higher burnup values (assemblies e5 to e8), whereas the highest peak corresponds to the four assemblies with the lowest burnup values (assemblies e1 to e4). In between, the k_{eff} values correspond to random mixtures of loadings.
To visualize the spread of k_{eff}, Fig. 8 presents the 70 combinations as a function of the averaged burnup of the 4 loaded assemblies. For each of these combinations, the spread of k_{eff} due to the axial and radial rotations is presented on the Y-axis. The cases with a circle indicate that at least one of the k_{eff} for the four

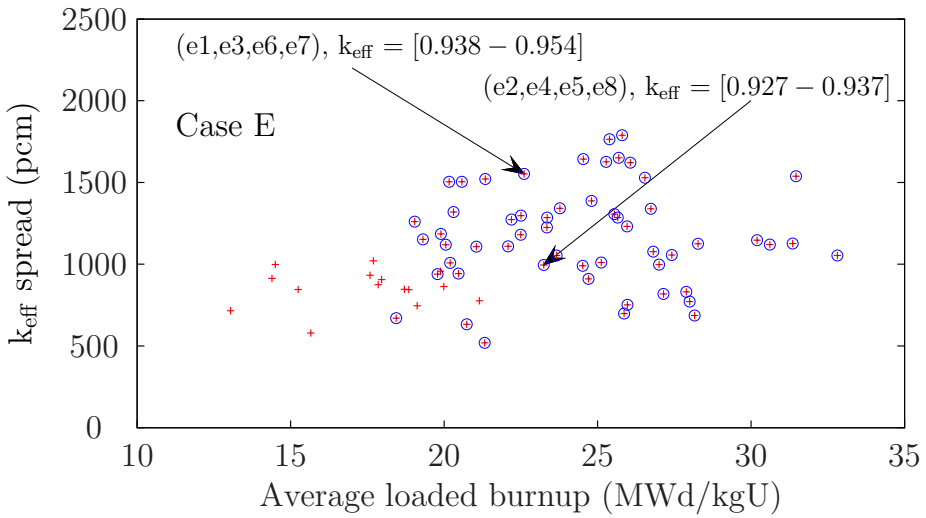

Fig. 8. Spread of k_{eff} for the considered combinations from case E. The cases with a blue circle indicate that the considered combination contain a k_{eff} value lower than 0.95 and is therefore allowed for loading. Two specific loadings are indicated, see text for details.

selected assemblies is lower than 0.95. Similarly to case D, the mixed loading allows to obtain loadings with $k_{eff} < 0.95$; the total impact of the radial and axial rotations can reach up to 2000 pcm, with up to 1200 pcm for the radial effect, and 1800 pcm for the axial effect. To present one loading solution for the 8 assemblies of case E in two canisters, an example is indicated in Fig. 8 with two arrows. The numbering of each loaded assembly corresponds to the ones in section 3.2.1. In the first canister, the assemblies e1, e3, e6 and e7 are

loaded, and the second canister contains the other assemblies (e2, e4, e5 and e8). For each canister, the selected assemblies can be rotated and the spread of k_{eff} is also presented in the figure. One can see that both minimum k_{eff} values for the two canisters are lower than 0.95. Additionally for the first canister, specific assembly rotations lead to k_{eff} values higher than 0.95. Other loadings also represent acceptable solutions.

In conclusion, both cases D and E are simulating various mixing of assemblies with different enrichment and burnup values. Such loadings are representative of the reality if the option of mixed loading with axial and radial rotations is allowed. Contrary to the homogeneous loading or to the simple mixed loadings (cases A to C), many possibilities lead to k_{eff} lower than 0.95 and the axial and radial rotation effects are important, as demonstrated.

4 Conclusion

This study fits in the context of optimizing the filling of canisters, and in making a better use of the available resources. We have demonstrated with a few examples that the mixed loading of canisters has advantages compared to the homogeneous one: from a criticality aspect, it allows to safely load assemblies with low and high burnup values in the same canister. Additionally, it was shown that in the case of the mixed loading, the axial and radial rotations can lower the k_{eff} by up to 2000 pcm, which is not the case for the homogeneous loading. In return, the irradiation history of each assembly needs to be known. Such results open the door of loading optimization of a full park of spent nuclear fuels. In Switzerland, about 12 000 assemblies will need to be safely and economically stored in the long-term repository. To that goal, one can apply the mixed loading to load assemblies with low burnup (for instance from the plant last cycle), or to obtain a uniform k_{eff} distribution, minimizing the difference between canisters. For that, the present work needs to be complemented by the use of metamodels (such as neural network and genetic algorithm), which can provide a estimated k_{eff} values in milliseconds. Such work is naturally complementing this study and is currently being performed. Finally, one also needs to keep in mind that other quantities, such as the decay heat, can play a key role for environmental protection. A realistic optimization will also need to take it into account.

References

[1] M. Elam and G. Sundqvist, "The Swedish KBS project: a last word in nuclear fuel safety prepares to conquer the world?", Journal of Risk Research **12** (2009) 969.

[2] M. Kojo, M. Kari, and T. Litmanen, "The Socio-Economic and Communication Challenges of Spent Nuclear Fuel Management in Finland: The Post Site Selection Phase of the Repository Project in Eurajoki," Progress of Nucl. Energy **52** (2010) 168.

[3] G. Spykman, "Dry storage of spent nuclear fuel and high active waste in Germany – Current situation and technical aspects on inventories integrity for a prolonged storage time", Nucl. Eng. and Techno. **50** (2018) 313.

[4] R. Patel, C. Punshon, J. Nicholas, P. Bastid, R. Zhou, C. Schneider, N. Bagshaw, D. Howse, E. Hutchinson, R. Asano and F. King, "Canister Design Concepts for Disposal of Spent Fuel and High Level Waste", Technical Report 12-06, October 2012, National Cooperative for the Disposal of Radioactive Waste, Switzerland.

[5] M.M. Gutierrez, S. Caruso and N. Diomidis, "Effects of materials and design on the criticality and shielding assessment of canister concepts for the disposal of spent nuclear fuel", Applied Radiation and Isotopes **139** (2018) 201.

[6] J.J. Herrero, A. Vasiliev, M. Pecchia, D. Rochman, H. Ferroukhi, L. Johnson and S. Caruso, "Criticality Safety Assessment for Geological Disposal of spent Fuel using the PSI BUCSS R Methodology", report NAB 17-23, October 2017, National Cooperative for the Disposal of Radioactive Waste, Switzerland.

[7] A. Vasiliev, J. Herrero, M. Pecchia, D. Rochman, H. Ferroukhi and S. Caruso, "Preliminary Assessment of Criticality Safety Constraints for Swiss Spent Nuclear Fuel Loading in Disposal Canisters", Materials **12** (2019) 494.

[8] D. Rochman, A. Vasiliev, H. Ferroukhi and M. Pecchia, "Consistent criticality and radiation studies of Swiss spent nuclear fuel: the CS_2M approach", Jour. of Hazardous Materials **357** (2018) 384.

[9] A.S. DiGiovine, J.D. Rhodes III, K.S. Smith, D.M. Ver Planck and J.A. Umbarger, "SIMULATE-3 Users Manual," Studsvik/SOA-95/15, Studsvik (1995).

[10] T. Simeonov and C. Wemple, "Update and evaluation of decay data for spent nuclear fuel analyses", proceedings of the International Conference on Nuclear Data for Science and Technology, ND2016, Bruges, Belgium, September 11-16, 2016, EPJ Web Conf. **146** (2017) 09011.

[11] T. Goorley, "*MCNP 6.1.1 - Beta release Notes*", Los Alamos National Laboratory, Report LA-UR-14-24680, June 2014.

[12] M. Pecchia, J.J. Herrero, H. Ferroukhi, A. Vasiliev, S. Canepa, A. Pautz, "COMPLINK: a versatile tool for automatizing the representation of material data in MCNP models", Proceedings of the Int. Conf. Nuclear Criticality Safety, ICNC 2015, Charlotte, NC, USA, September 13-17, 2015.

[13] "Inside Bill's brain: Decoding Bill Gates", Part 2, 2019, Documentary by D. Guggenheim.

[14] "Burn-up Credit Criticality Studies, Benchmark Analyses for Pressurised Water Reactors", Report of the OECD Nuclear Science, NEA/NSC/R(2016)1, September 2016.

[15] "Optimization Strategies for Cask Design and Container Loading in Long Term Spent Fuel Storage", IAEA report TECDOC-1523, Decemebr 2006.

[16] "Spent nuclear fuel for disposal in the KBS-3 repository", SKB Technical Report TR-10-13, December 2010.

[17] H. Ralko, "Canister Design 2012", Posiva technical report POSIVA 2012-13, April 2013.

[18] M. Anttila, "Criticality Safety Calculations for Three Types of Final Disposal Canisters", Posiva technical report POSIVA 2005-13, July 2005.

[19] K. Yamamoto, H. Akie and K. Suyama, "A study on the criticality safety for the direct disposal of used nuclear fuel in Japan: application of burnup credit to the criticality safety evaluation for the disposal canister", proceedings of the International Conference on Nuclear Criticality Safety, p. 228, Charlotte, NC, USA, September 13-17, 2015.

[20] D. Damalet, R. Giraud, G. Sacre and L. Bindel, "Criticality safety analysis of spent fuel storage or handling disposals using burnup credit - loading curve calculation", proceedings of the International Conference on Nuclear Criticality Safety, p. 574, Charlotte, NC, USA, September 13-17, 2015.

[21] J.C. Wagner and C.E. Sanders, "Assessment of Reactivity Margins and Loading Curves for PWR Burnup-Credit Cask Designs", Oak Ridge National Laboratory Technical report NUREG/CR-6800, ORNL/TM-2002/6, March 2003.

[22] "Costing of Spent Nuclear Fuel Storage", IAEA Nuclear Energy Series No. NF-T-3.5, International Atomic Energy Agency, Vienna, 2009.

[23] E. Vlassopoulos, B. Volmert and A. Pautz, "Logistics optimization code for spent fuel loading into final disposal canisters", Nucl. Eng. and Design **325** (2017) 246.

[24] J. Rhodes, K. Smith and D. Lee, CASMO-5 development and applications, Proceedings of the PHYSOR-2006 conference, ANS Topical Meeting on Reactor Physics, Vancouver, BC, Canada, September 10-14, Vancouver, BC, Canada, September 10-14, 2006, p. B144.

[25] E. Fuentes, D. Lancaster, C. Kang and W. Lake, "Actinide-Only Burnup Credit for Spent Fuel Transport", International Journal of Radioactive Materials Transport **9** (2013) 249.

[26] J. Leppänen. "Serpent - a Continuous-energy Monte Carlo Reactor Physics Burnup Calculation Code", VTT Technical Research Centre of Finland. (June 18, 2015).

[27] H. Ferroukhi, K. Hofer, J.M. Hollard, A. Vasiliev and M. A. Zimmermann, "Core Modelling and Analysis of the Swiss Nuclear Power Plants for Qualified R&D Applications" in the Proceedings of the Int. Conf. on the Physics of Reactors, PHYSOR'08, Interlaken, Switzerland , 2008.

[28] J.J. Herrero, M. Pecchia, H. Ferroukhi, S. Canepa, A. Vasiliev, S. Caruso, "Computational Scheme for Burnup Credit applied to Long Term Waste Disposal", Proceedings of the Int. Conf. Nuclear Criticality Safety, ICNC 2015, Charlotte, NC, USA, September 13-17, 2015.

[29] J.J. Herrero, D. Rochman, O. Leray, A. Vasiliev, M. Pecchia, H. Ferroukhi, S. Caruso, "Impact of nuclear data uncertainty on safety calculations for spent nuclear fuel geological disposal", Proceedings of the Int. Conf on Nuclear Data 2016, ND2016, Bruges, Belgium, September 11-16, 2016.

[30] T. Ranta and F. Cameron, "Heuristic Methods for assigning spent nuclear fuel assemblies to cansiters for final disposal", Nucl. Sci. and Eng. **171** (2012) 41.

[31] G. Zerovnik, L. Snoj and M. Ravnik, "Optimization for spent nuclear fuel filling in canisters for deep repository", Nucl. Sci. and Engineering **163** (2009) 183.